REINFORCEMENT IMPACT ON STATE OF CRACKS IN CONCRETE SLABS

Volodymyr Bulgakov[1], Oleksii Kutsenko[2], Anastasiya Kutsenko[1], Aivars Aboltins[3], Semjons Ivanovs[3]
[1]National University of Life and Environmental Sciences of Ukraine, Ukraine;
[2]Taras Shevchenko National University of Kyiv, Ukraine;
[3]Latvia University of Life Sciences and Technologies, Latvia
aivars.aboltins@lbtu.lv, semjons@apollo.lv

Abstract. In the present work the stress-strain state of a reinforced concrete slab with a transverse edge crack of constant depth is considered. There is investigated the effect of reinforcement upon the distribution of the fracture mechanics along the crack front. The uniformly or linearly distributed stresses at the slab ends are described as an external load. These loads correspond to pure tension and pure bending of the slab, respectively. For a case when the depth of the crack is less than the depth of the reinforcement rod, an analytical approach for an assessment of the crack state is proposed. As a characteristic of the crack state, the stress intensity factor (SIF) is used. Using the finite-element CalculiX package, the numerical results have been obtained, and adequacy of the analytical solution justified. The calculations have been performed for a wide range of variations in the geometrical parameters of the slab and the crack. For this purpose, a principle of replacing the external load with the pressure on the crack faces, well known in linear fracture mechanics, is generalized for the case of heterogeneous elastic bodies. The results of calculations show that the variation of the SIF value along the crack front is insignificant (up to 5% for practically realizable parameter values). On this basis it is concluded that the crack depth most likely is constant in the early stages of its fatigue development. For shallow cracks the SIF value will decrease near the reinforcing rod. It is interesting to note that for deep cracks the presence of reinforcement can lead to local increasing, not decreasing, of the SIF values. Considering this fact, the results presented in the paper may be useful in the design of reinforced concrete structures. It is especially important to take it into account in an individual design, in particular, in designing agricultural buildings where non-standard reinforced concrete structures are used.

Keywords: reinforced concrete slab, tension, bending, stress intensity factor, analytical solution.

Introduction

Since most modern building structures include reinforced concrete elements, the importance of studying the crack resistance of these elements is beyond doubt. One of the most common structural elements are reinforced concrete slabs. A lot of works are devoted to the research of crack resistance of reinforced concrete elements. The main emphasis in these works is placed on studying the crack resistance properties of concrete as a material. An overview of the directions of development of these studies can be found in [1; 2]. A relatively small part of works is devoted to the study of the interaction of concrete and reinforcement, more precisely, the study of the effect of reinforcement upon the state of cracks in concrete. A recent extensive review of the corresponding papers can be found in [3]. But even in these works (see, for example, [4]), there are considered, as a rule, certain configurations of reinforced concrete elements, which makes it impossible to generalize their results for a wide range of the existing reinforced concrete elements, including reinforced concrete slabs.

Although concrete is a non-linear material, there are confirmations of the possibility of using linear elastic fracture mechanics (LEFM) to study its crack resistance. It was demonstrated in [5] that the applicability of LEFM depends on the dimensions of the concrete element and the allowable values for various types of deformation were given. There are also examples of successful practical application of LEFM methods to concrete structures (see, for example, [6]). These methods make it possible to assess the state of cracks for a wide range of changes in the geometric and physical parameters of the reinforced concrete elements. Taking into account the regularities of the impact of reinforcement upon the state of cracks, obtained in this way, helps increase the crack resistance of the reinforced concrete elements. This is especially important under the conditions of rural low-rise construction where individual construction projects are often implemented, and non-standard reinforced concrete elements are used.

This work is a continuation of the research, started in [7]. But a fundamental difference of this work with [7] is the assumption that the crack did not reach the reinforcement ($l < a$), i.e. the crack faces and the reinforcing rods (bars) do not intersect. Therefore, we consider a concrete rectangular slab of the length L, width W and thickness h, reinforced with longitudinal steel rods with a step $2s$ along the width of the slab (Fig. 1). The axes of the reinforcing rods are located at a distance a from the bottom surface of the slab, and their diameter is d. It is assumed that in a certain cross section of the slab there is a face

crack of constant depth *l*, the faces of which do not reach the reinforcing rods: $l < a - d/2$ (Fig. 2). The problem is how to determine the distribution of the stress intensity factor (SIF) along the crack front in tension and bending of the slab for various values of geometric parameters. As it is known [8], SIF is the main characteristic of the linear fracture mechanics. Due to the periodicity and symmetry, in order to solve the problem, it is sufficient to consider one half-period of the slab with a width of *s*.

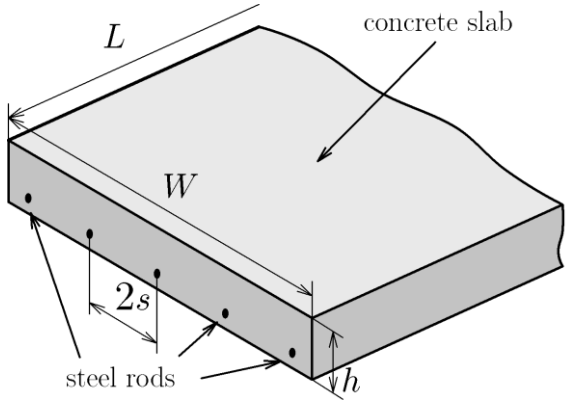

Fig. 1. **General view of slab**

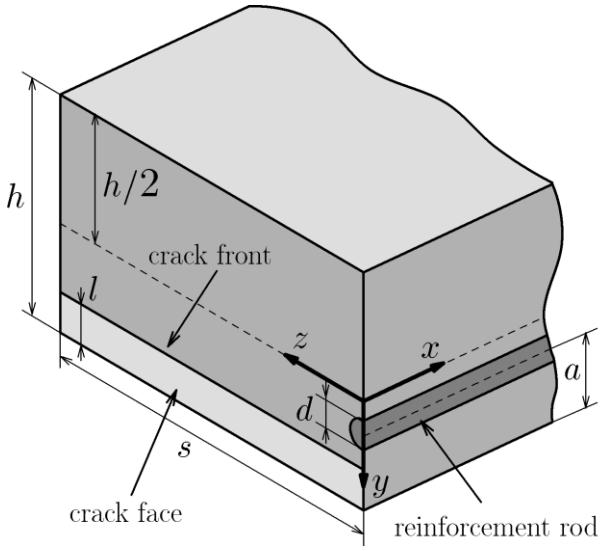

Fig. 2. **Half-period of slab**

Materials and methods

To assess the state of a crack, it is first necessary to perform an analysis of the stress-strain state of a reinforced slab without cracks. The period of such a slab is a composite rod, consisting of a reinforcing rod and a concrete matrix. The theory of tension and bending of composite rods, based on the Euler-Bernoulli hypothesis, is well developed and included into many textbooks on the strength of materials and the theory of elasticity (see, for example, [9]). Let us expose its main provisions, necessary for constructing an analytical solution.

The starting point in obtaining expressions for stress is the Euler-Bernoulli kinematic hypothesis: initially flat sections, orthogonal to the axis of the rod, remain flat and orthogonal to the axis of the rod even after its deformation. As a composite rod, we will consider the slab period, which includes one reinforcing rod. In this case, the period axis is parallel to the axis of the reinforcing rod.

In the case of pure stretching the period axis does not change its configuration. Therefore, the hypothesis of flat cross sections means that the sections move rectilinearly along the axis as absolutely rigid. It follows from this that the longitudinal deformations of the concrete matrix ε_c and the reinforcement ε_s coincide. Due to the relative smallness of the slab thickness the normal stresses in the axial direction y can be neglected in both components of the slab, while in the direction z (the plate width) the normal stresses can be neglected only in the reinforcing rod, but in the concrete matrix it is correct to consider the corresponding deformation component as absent.

$$\varepsilon_c = \frac{1-\nu_c^2}{E_c}\sigma_c = \frac{\sigma_c}{\bar{E}_c}, \quad \varepsilon_s = \frac{\sigma_s}{E_s}, \tag{1}$$

where E_c, E_s – elasticity moduli of concrete and steel;
ν_c – Poisson's ratio of concrete;
$\bar{E}_c$ – reduced modulus of elasticity of concrete;
σ_c, σ_s – longitudinal stresses in the concrete matrix and the reinforcing rod.

The values of stresses σ_c and σ_s are found from the equilibrium condition of the period of the slab. Obviously, the cross-sectional area of the entire period *A*, the cross-section of the reinforcing rod A_s and the cross-section of the concrete matrix A_c are given by the correlations

$$A = 2sh,\ A_s = \frac{\pi d^2}{4},\ A_c = A - A_s.$$

Assuming that uniformly distributed constant axial stresses p are set at the end of the slab (see Fig. 3a), then the equilibrium equation for the period of the slab in the projection of all forces in the longitudinal direction can be written as

$$A_c\sigma_c + A_s\sigma_s = A\,p. \tag{2}$$

From (2), taking into account (1), we find (3)

$$\sigma_c = \frac{\overline{E}_c A}{\overline{E}_c A_c + E_s A_s}\,p,\ \sigma_s = \frac{E_s A}{\overline{E}_c A_c + E_s A_s}\,p. \tag{3}$$

Correlations (3) determine the stress state in the reinforced slab without cracks when it is stretched.

By virtue of the Saint-Venant principle they are performed at a distance from the ends of the slab with a value of several its thicknesses. Since the value of the elasticity modulus of steel is an order greater than the value of the elasticity modulus of concrete, the stresses in the reinforcing rod are also an order higher than the stresses in concrete.

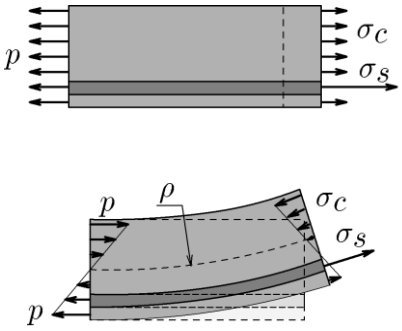

Fig. 3. **Stress distribution at slab under:** a – tension; b – bending

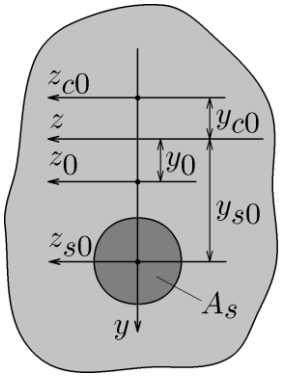

Fig. 4. **Geometry of slab cross-section near arming rod**

At pure bending the kinematics of the cross-sections period is more complicated: while remaining flat, they turn by a certain angle (see Fig. 3b). Besides, the axis of the period becomes curved along the arc of the circle in plane $x\,y$. As in the case of the homogeneous rod, the consequence of the hypothesis of flat sections is a linear distribution of stresses along the coordinate:

$$\sigma_c = \overline{E}_c\,\frac{y - y_0}{\rho},\ \sigma_s = E_s\,\frac{y - y_0}{\rho}, \tag{4}$$

where ρ – radius of curvature of the period axis after deformation;
y_0 – coordinate y of the centre of the cross-sectional area of the period (the period axis).

The position of the period axis is found from the condition of absence of the longitudinal force:

$$\int_{A_c} \sigma_c\,dA + \int_{A_s} \sigma_s\,dA = 0. \tag{5}$$

Substituting (4) into (5), after obvious transformations, we obtain an expression for the coordinate of the period axis:

$$y_0 = \frac{\overline{E}_c S_c + E_s S_s}{\overline{E}_c A_c + E_s A_s} = \frac{\overline{E}_c A_c y_{c0} + E_s A_s y_{s0}}{\overline{E}_c A_c + E_s A_s},$$

where S_s, S_c – static moments of the cross sections of the reinforcing rod and the concrete matrix relative to axis z, equal to the product of their areas A_s and A_c by the coordinates of their own centres y_{s0} and y_{c0} (see Fig. 4).

The value of the radius of curvature of the period axis after deformation is found from the equilibrium condition for the moment of all forces relative to axis z:

$$\int_{A_c} \sigma_c y\, dA + \int_{A_s} \sigma_s y\, dA = M\ , \tag{6}$$

where M – bending external moment.

Taking into account (4), equation (6) makes it possible to express the radius of curvature in terms of the bending moment:

$$\frac{1}{\rho} = \frac{M}{\overline{E}_c I_c + E_s I_s}\ ,$$

where I_s, I_c – moments of inertia of the cross sections of the reinforcing rod and the concrete matrix relative to the central axis of the entire cross section z_0. This axis passes through point $y = y_0$ parallel to the axis z (see Fig. 4).

Consequently, at a pre-set bending moment for one period of the slab the longitudinal stresses have the following distributions:

$$\sigma_c = \frac{M\, E_c}{\overline{E}_c I_c + E_s I_s}\left(y - y_0\right),\ \sigma_s = \frac{M\, E_s}{\overline{E}_c I_c + E_s I_s}\left(y - y_0\right). \tag{7}$$

Correlations (7) determine the stress state in a reinforced slab without cracks far from the ends of the slab during its pure bending. If the bending moment at the end is given in the form of linearly distributed longitudinal stresses, then its value is determined by the formula

$$M = \int_A \sigma y\, dA = \frac{2p}{h}\int_A y^2 dA = \frac{h^2 s}{3}\, p\ ,$$

where p – maximum value of longitudinal stresses at the end of the slab (see Fig. 3b).

Knowledge of the stress state in a slab without cracks makes it possible to construct an analytical method to determine the characteristics of a crack in its presence. As a parameter, characterizing the state of the crack, we will use the stress intensity factor (SIF). Since the crack is located entirely in the concrete matrix, to find SIF distribution along its front, one can use numerous analytical dependencies, given for homogeneous bodies in the reference literature. In addition, the external load for a homogeneous period (without a reinforcing rod) will not coincide with the external load for the period of the considered reinforced concrete slab. It is chosen from the considerations that in both cases the stress state on an imaginary, mentally drawn surface of the crack faces must coincide. For example, in the case of pure tension of the initial period by stresses, the period p without reinforcement should be stretched by stresses σ_c, determined by the first of formulas (3) (see Fig. 3a).

In accordance with correlations (3) and (7), the longitudinal stresses on the imaginary crack faces of the initial period take either constant values or values that vary linearly with the depth.

Besides, these stresses do not change along the crack front. Therefore, to further construct an analytical solution, one can use the expressions for SIF for an edge crack in an elastic strip, stretched by constant and linearly varying stresses. The corresponding approximations can be found in the handbook [10]. So, for the case of pure tension it contains an approximation of the values of the stress intensity factor K_I, which in our notation can be presented as

$$K_I = \sigma_c \sqrt{\pi l}\left(1.12 - 0.231\alpha + 10.55\alpha^2 - 21.72\alpha^3 + 30.39\alpha^4\right),\ \alpha = l/h\,. \tag{8}$$

The relative error of such an approximation does not exceed 0.5% for $\alpha \le 0.6$.

To determine SIF for pure bending, the stress in (7) must be decomposed into constant and linearly proportional components:

$$\sigma_c = \sigma_{c0} + \sigma_{c1}\frac{y}{h/2},\ \sigma_{c0} = -\frac{M\,\overline{E}_c}{\overline{E}_c I_c + E_s I_s}\, y_0,\ \sigma_{c1} = \frac{M\,\overline{E}_c}{\overline{E}_c I_c + E_s I_s}\frac{h}{2}\,.$$

For the constant component approximation (8) is again used, replacing in it σ_c. For the linearly proportional component we can use approximation [10]

$$K_I = \sigma_{c1}\sqrt{\pi l}\left(1.122 - 1.4\alpha + 7.33\alpha^2 - 13.08\alpha^3 + 14.0\alpha^4\right),\ \alpha = l/h, \quad (9)$$

the relative error of which does not exceed 0.2% for $\alpha \leq 0.6$. The calculated value of SIF in this case is found as the sum of (8) and (9).

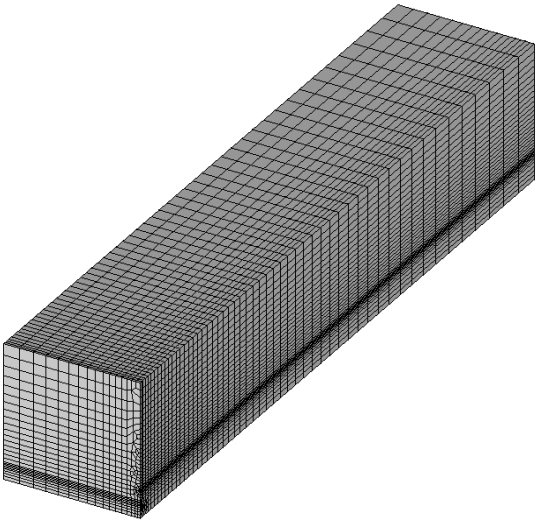

Fig. 5. **General view of finite element model for $\bar{s}$ = 1, $\bar{l}$ = 0.1, $\bar{a}$ = 0.2, $\bar{d}$ = 0.05**

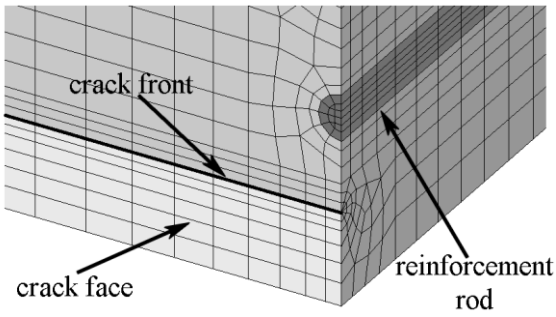

Fig. 6. **Part of the model with crack face zone near reinforcement rod**

To test the proposed analytical approach, calculations were carried out, using the CalculiX finite element package [11]. This package has proven itself well in solving problems of fracture mechanics [12]. To perform calculations, a multi-parameter finite-element model was built.

As the main geometric parameters, the depth of the crack *l*, the depth of the axis of the reinforcement rod *a* , the diameter of the reinforcement rod *d* and the length of the half-period *s* were determined. All of them were dimensionless by their ratio to the plate thickness. The model was built for a large number of values of these parameters. The values of the dimensionless crack depth $\bar{l}$ and the dimensionless depth of the reinforcing rod axis $\bar{a}$ were moved in increments of 0.1, the dimensionless diameter of the rods $\bar{d}$ was taken equal to 0.05 and 0.1, and the dimensionless length of the half-cycle $\bar{s}$ was taken to be 1 and 2. The general view and a fragment of the model are shown in Figures 5 and 6, respectively.

Results and discussion

Examples of distribution of longitudinal stress fields in the half-period of the slab in tension and bending, calculated by the finite element method, are shown in Figures 7, 8 and 9, 10, respectively. The following values of elastic characteristics were taken in calculations: E_c = 24GPa, E_s = 210GPa, v_c = 0.2, v_s = 0.3. It can be concluded from Figure 7 that during tension over the entire cross section of the crack, with the exception of points, adjacent to the crack front and the reinforcing rod, practically constant longitudinal stresses act in the concrete matrix. Similarly, it follows from Figure 9 that the stresses in bending are generally distributed linearly. In addition, Figures 8 and 10 show that in both cases the level of longitudinal stresses in the reinforcing rod is much higher. Thus, the numerical calculations confirm the adequacy of distributions (3) and (7).

The results of the numerical calculation of SIF, in comparison with the values analytically determined by formulas (8) and (9), are shown in Figures 11-14. In all these graphs the solid lines correspond to the numerical values of SIF, and the dashed lines correspond to the analytical ones. Also, the values of the parameters $\bar{d}$ = 0.05 and $\bar{s}$ = 1 are chosen as common for all graphs. The numbers in the circles represent the values of the parameter $\bar{a}$, corresponding to the curve. The horizontal axis shows the dimensionless frontal coordinate: $\bar{z} = z/s$, and the vertical axis shows the dimensionless value

$$\overline{K} = \frac{K}{p\sqrt{l}}$$

of SIF. The subscript “N” means that SIF was calculated when the slab was stretched, and the index “M” was calculated when it was bent. Consequently, Figures 11 and 12 show the SIF distributions for the case of tension, and Figures 13 and 14 for the case of bending.

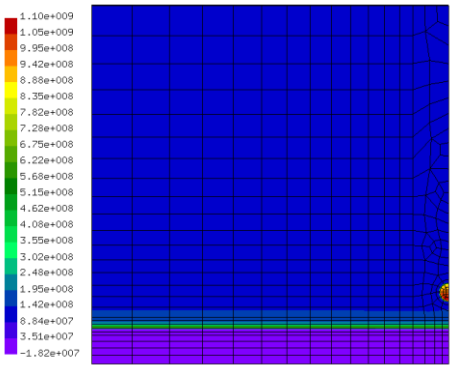

Fig. 7. **Stress distribution over the cross-section of crack location (tension)**

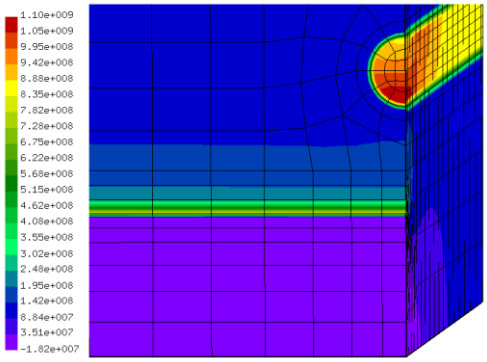

Fig. 8. **Stress distribution within “crack face - reinforcement rod” zone (tension)**

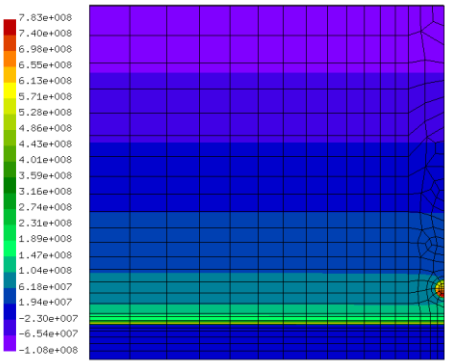

Fig. 9. **Stress distribution over the cross-section of crack location (bending)**

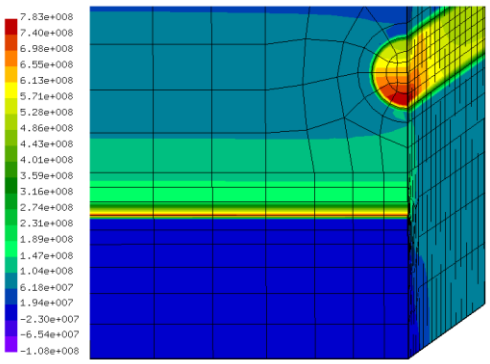

Fig. 10. **Stress distribution within “crack face - reinforcement rod” zone (bending)**

Figure 11 presents the plots of distribution of SIF in tension of the slab for a crack of depth $\overline{T} = 0.1$ at different depths of the axis of the reinforcing rod. For each value of the second parameter its own curve is numerically constructed, while the analytical value of SIF does not depend on it, and, therefore, there is only one dashed curve. At a first glance on the figure, it can make the impression of a significant scatter of the obtained values. However, in fact, the relative width of the interval of change of all values is less than 5%. If the vertical scale were set off from its zero value, it would be difficult to distinguish the curves in the graph scales. This conclusion applies to all presented graphs, and to the results obtained, in general. Thus, one can reveal good agreement between the calculated and the analytical values of SIF. The local impact of the reinforcing rod upon the SIF values is manifested when the crack front approaches the reinforcing rod at a distance, comparable to its diameter. The plots of the distribution of SIF at the slab tension for a crack of the depth $\overline{T} = 05$ and different depths of the reinforcing rod axis are presented in Figure 12. The conclusions, drawn on the basis of the analysis of the graphs in Figure 11, remain valid in this case as well. Comparison of the graphs in Figures 11 and 12 shows that the sensitivity of the SIF values to the closely spaced reinforcement for deep cracks is somewhat higher.

Figures 13 and 14 present graphs of SIF distribution at bending of the slabs containing cracks with the depth $\overline{T} = 0.1$ and $\overline{T} = 0.5$. At bending, in contrast to the case of tension, the stresses in the concrete matrix (7) depend on the depth of the reinforcing rod, so each solid curve has its own dashed curve. On the whole, agreement between the numerical and the analytical results in the case of bending is even better than in the case of tension. At the same time there is also a lower sensitivity of the SIFvalues to

the location of the reinforcement. It is interesting to note the fact (see Fig. 14) that for deep cracks, when the reinforcing rods are laid on the side of the compressed fibers of the slab, they can even cause a slight increase in the SIF values, i.e. contribute to the destruction of concrete.

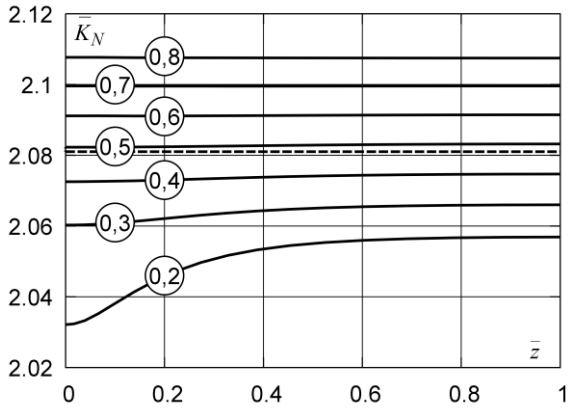

Fig. 11. **SIF for $\bar{T}$ = 0.1 (tension)**

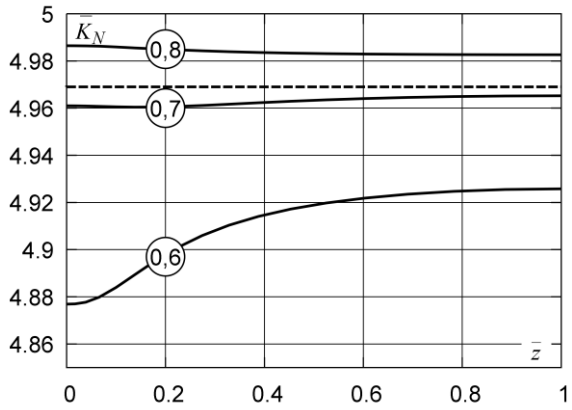

Fig. 12. **SIF for $\bar{T}$ = 0.5 (tension)**

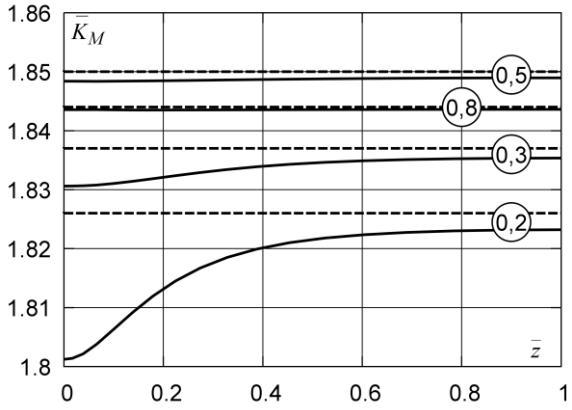

Fig. 13. **SIF for $\bar{T}$ = 0.1 (bending)**

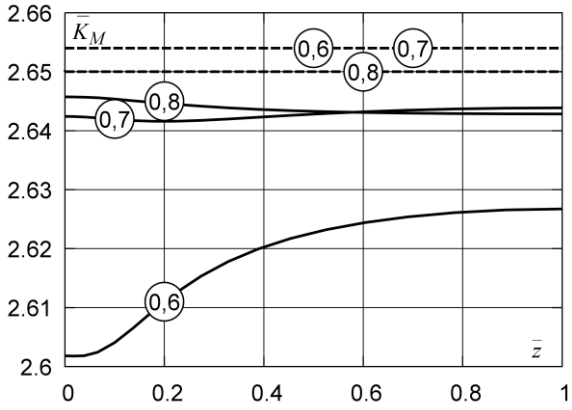

Fig. 14. **SIF for $\bar{T}$ = 0.5 (bending)**

Conclusions

The calculation results show that the impact of the reinforcing rod upon the change in the SIF value along the crack front can be neglected when the distance between them is the diameter of one rod, or more. In this case, the corresponding constant SIF value can be calculated with high accuracy, using the analytical formulas, provided in this work. This conclusion is valid both for the case of the slab tension and for the case of its bending. It follows from what has been said that at the initial stages of development of cracks in the reinforced concrete slabs, their depth also practically does not change along the crack front if the factors, other than the mechanical load, do not influence the process of the crack development.

When the crack front approaches the reinforcing rod, its impact manifests itself in the form of local decrease in the SIF value for shallow cracks (up to half the thickness of the slab). In the case of deep cracks, the reverse phenomenon can be observed - as the crack front approaches the reinforcing rod in its vicinity, the SIF value increases. This conclusion indicates the inadmissibility of using reinforced concrete slabs in an “inverted” state when reinforcement is in the upper layers of the slab. In addition to the obvious loss of strength in such a position, such slab also reduces the crack resistance. Moreover, in order to increase the crack resistance of a slab with a two-layer reinforcing frame, the upper reinforcing rods should be chosen with a smaller diameter than the lower rods. This recommendation is relevant within the context of rural buildings, since the implementation of individual construction projects often uses elements of the same type.

Author contributions

All the authors have contributed equally to creation of this article.

References

[1] Kumar S., Barai S. Concrete Fracture Models and Applications. – Berlin: Springer-Verlag, 2011, 262 p.
[2] Akram A. The overview of fracture mechanics models for concrete. Architecture Civil Engineering Environment, Vol. 14, №1, 2021, pp. 79-89.
[3] Zhang P., Wang C., Gao Z., Wang F. A review on fracture properties of steel fiber reinforced concrete. Journal of Building Engineering, Vol. 67, 2021, pp. 1-23.
[4] Malipatil K., Itti S. Stress intensity factor and damage index of reinforced concrete beam. Proceedings of Fatigue Durability India 2019, Belagavi, 2019, pp. 305-316.
[5] Bazant Z.P., Planas J. Fracture and Size Effect in Concrete and Other Quasibrittle Materials. – New York: Routledge, 1998, 640 p.
[6] Chauhan D.R., Tewani H.R., Kalyana Rama J.S. Application of Principles of Linear Elastic Fracture Mechanics for Concrete Structures: A Numerical Study. Applied Mechanics and Materials, Vol. 877, 2018, pp. 282-288.
[7] Kutsenko A., Kutsenko O. Effect of Reinforcement on the Crack Resistance of Concrete Slabs. Machinery & Energetics, Vol. 13, №3, 2022, pp. 34-42.
[8] Zrazhevsky G., Kepich T., Kutsenko O. Basics of the theory of strength, deformation and fracture mechanics. – Kyiv: LOGOS, 2005. 169. (In Ukrainian).
[9] Ugural A.C., Fenster S.K. Advanced Mechanics of Materials and Applied Elasticity. – New York: Prentice Hall, 2019, 752 p.
[10] Murakami Y. (ed.) Stress Intensity Factors Handbook. Vol. 2. – Oxford: Pergamon Press, 1987, 1456 p.
[11] Dhondt G. The Finite Element Method for Three-Dimensional Thermomechanical Applications. – Hoboken: Wiley, 2004, 340 p.
[12] Bulgakov V., Aboltins A., Kutsenko O., Ivanovs S., Pascuzzi S. Approximate approach of research and assessment of crack resistance of cylindrical housings. 20th International Scientific Conference. Engineering for Rural Development, Jelgava, Latvia, 2021, pp. 1541-1547.